INTERANNUAL VARIATIONS IN THE RETREAT OF THE NOTHERN SEASONAL CAP OF MARS USING COMPUTER VISION. P. J. Acharya[1] (4700 Keele St, Toronto, ON M3J 1P3, pruthvi1@yorku.ca), I. B. Smith[1] (ibsmith@yorku.ca), and W. Calvin[2] (wcalvin@unr.edu), [1]York University, Toronto, Ontario, Canada, [2]Nevada University, Reno, Nevada

Introduction: One of the largest features on Mars is the Northern Seasonal Polar Cap (NSPC), with can cover up to 12% of the surface seasonally [1]. The NSPC condenses up to 25% of the atmosphere during wintertime and releases it during springtime [2], leading to a major change in the global atmospheric pressure and composition. Intense atmospheric activities are often seen originating near the cap's edge during springtime [3,4]. These activities have been seen to reach very close to the equator, indicating a large amount of material being moved in and out of the polar region. For these reasons, it's critical to understand the NPSC's recession to understand the past, current, and future Martian climate.

The focus of this work was to update and extend the previously published results [4] using an automated approach. We were able to track the cap's edge at a higher temporal resolution than previously possible [4] and were able to add new MYs that haven't been analyzed previously. With the enhanced dataset, w determined the seasonal variation in the recession rate for each year, interannual observations, and mid-season changes that were previously undetected.

MARCI Observations: We used large-scale visual observations from the Mars Color Imager (MARCI) from MY 29 to MY 35. Each observation is a mosaic of 12-13 images taken within 24 hours, each image covers ~27.7º of the northern polar region (Fig 1a) [4]. For each MY, we tracked the cap until L_s = 70º; around this time the cap's edge reaches the polar layered deposits and it's difficult to distinguish between the seasonal and residual ice.

Automated Tracking: Using Python and an open-sourced computer vision library called OpenCV, we automated outlining the cap and fitting an ellipse of best fit. Our method relied on using the HSV color format, where important properties of color are decoupled into their own channels. Using this format, empirically determined the best upper and lower H, S, and V bounds that best outlined the seasonal cap and ignored the water-ice clouds (Fig 1b,c). Then we fitted an initial ellipse best fit (Fig 1a) and used a simple filtering algorithm to remove any outlier outline points, which were caused by imaging artifacts (Fig 1d) and dust storms (Fig 1e), to get a filtered ellipse fit. We record the semi-major axis and the area of the ellipse fits and used over 95% of the total MARCI observations. Our new method was significantly faster and produced a higher temporal resolution curve compared to the previous approaches using the same MARCI dataset (Fig 2b) [4].

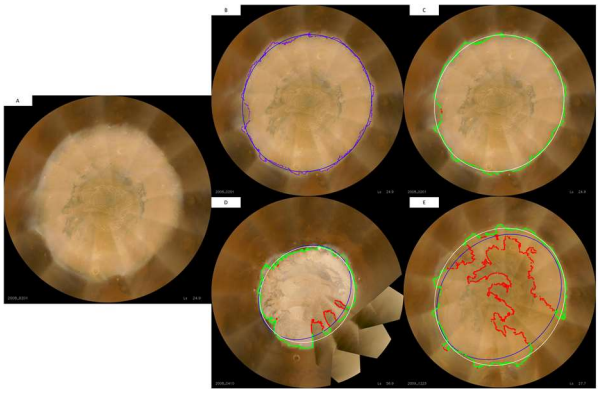

Figure 1: A. *shows the RGB MARCI mosaic at MY 29 L_s = 24.9º.* ***B.*** *shows the MARCI mosaic at MY 29 L_s = 24.9º with the initial ellipse fit (Blue) and outline points (Purple).* ***C.*** *shows the MARCI mosaic at MY 29 L_s 24.9º with the filtered ellipse (White), outline points that passed the filtering algorithm (Green), and points that failed (Red).* ***D.*** *shows the MARCI mosaic at MY 29 L_s = 56.9º during an imaging artifact.* ***E.*** *shows MARCI the mosaic at MY 30 L_s = 27.7º during a dust storm.*

Validation: We compared our outline and latitude points with previously published results, who manually tracked the cap [4], to verify our method and found very similar outlines (Fig 2a) and fits that produced similar recession rates; however, our latitude points were at most ~1º smaller due to the difference in the best-fit shape (ellipse vs circle) (Fig 2b). When we imposed a circle of best fit onto our outline, the maximum difference decreased to ~0.33º, and many MYs showed no difference between the two methods. We chose an ellipse fit because the cap became asymmetrical during late spring, and an ellipse fit, with its higher degrees of freedom, was a better fit for the non-circular cap.

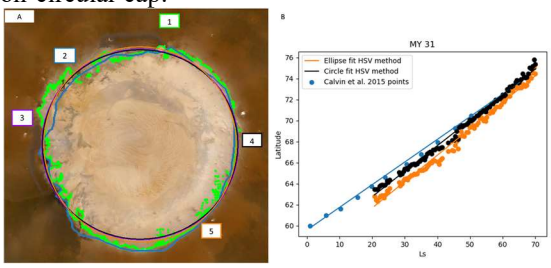

Figure 2: A. *Comparing (1) our outline, (2) previous published outline, (3) previously published circle of best fit, (4) our circle of best fit, (5) our ellipse of best fit at MY 29 L_s = 62º.* ***B.*** *Comparing our recessional trends, circle of best fit (Black), and ellipse of best fit (Orange), with previously published results (Blue).*

Results: We used a line of best fit, a 7th order polynomial fit and its first derivative to analyze the

multi-year average and individual MY recession curves. We found that most MYs behaved very similar to each other, with an average recession rate of ~0.24º/L_s. Most MYs diverged from the linear rate between L_s = ~35º and L_s = ~50º, transiting from the annual minimum to maximum recession rate.

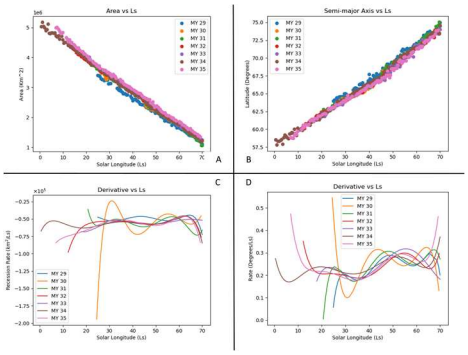

Figure 3: ***A.*** *Area trends for MY 29 to MY 35.* ***B.*** *Latitude trends for MY 29 to MY 35.* ***C.*** *Area recession rate trends for MY 29 to MY 35.* ***D.*** *Latitude recession rate trends for MY 29 to MY 35.*

Sudden Latitude Increasing Event: We observed that MY 29 and MY 30 experienced a sudden increase in their latitude during mid to late spring lasting ~2º L_s dates, followed by ~4º L_s dates where recession halted. We found that the recession rate after this sudden increase went up by ~35% (Fig 4a,b) and a small dust storm at ~330ºE around the time of the increase (Fig 4c,d).

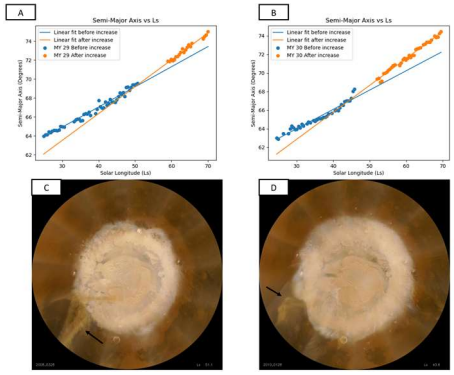

Figure 4: ***A.*** *shows the latitude vs L_s for MY 29 with the linear fit before (Blue) and after (Orange) sudden increase.* ***B.*** *shows the latitude vs L_s for MY 30 with the linear fit before (Blue) and after (Orange) sudden increase.* ***C.*** *shows a dust storm occurring at MY 29 L_s = 51.1º around the time of the increase.* ***D.*** *shows a dust storm occurring at MY 30 L_s = 43.6º around the time of the increase.*

We believe that the sudden increase may be caused by a major sublimation event and katabatic winds flowing away from the pole (Fig 5b). After this, recession halts because the cap's edge is sufficiently far away from the Sun's maximum latitude reach and won't resume until the Sun catches up to the cap's edge (Fig 5c). Once the Sun reaches the cap's edge, recession resumes but it is enhanced by katabatic winds, which are stronger than before and known to increase sublimation rates [5,6,7,8] (Fig 5d).

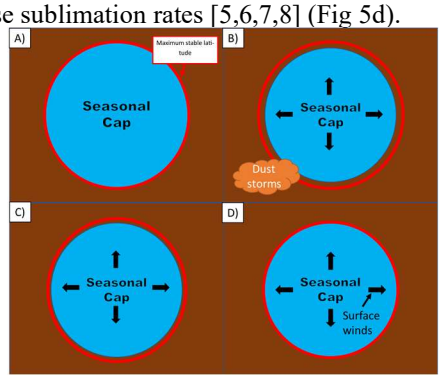

Figure 5: *Timeline of the sudden latitude increasing event. The blue circle represents the seasonal cap, the red circle represents the maximum latitude where the cap is stable or maximum latitude reach of the Sun, and black arrows represent the katabatic winds.* ***A.*** *Cap receding solely due to solar radiation and closely following the maximum stable latitude.* ***B.*** *A major sublimation event decreases the size of the cap and seasonal katabatic winds formed during this time, causing the storms seen around this time.* ***C.*** *Recession halts because the cap is well within the stable latitude region and katabatic winds are sufficient to continue recession.* ***D.*** *Maximum stable latitude reaches the cap's edge and recession resumes but is enhanced by katabatic winds.*

Effects of the Global Dust Storms: We found that the area trends for the two post-global dust storm years, MY 29 and MY 35, differed from the multi-year average. MY 29's area was significantly smaller and receded slower than the multi-year average until L_s = ~45º. Similar behavior was observed using spectral observations; however, it showed that the cap was smaller and receded slower than average until L_s = ~35º [1]. MY 35's area was larger than the multi-year average, but it decreased it at the average rate. We believe that the difference in the timings of the two storms, MY 28 and MY 34 storms, are the primary cause for the diverging behavior. One possibility is that the late MY 28 storms [1,9] may have displaced the polar vortex [1], causing portions of the cap to sublimate faster than others [1]. For the early MY 35 storms [9], one possibility is that the formation rate may have been enhanced by the colder than average surface present after the storms [10].

Acknowledgments: We gratefully acknowledge the support of the NSERC Discovery grant to IBS and from the Technology for Exo-Planetary Science (TEPS) CREATE grant to PA

References: [1] Piqueux, S. et al. (2015) Icarus, 251, 164–180. [2] Tillman, J. E.et al. (1993) JGR 98(E6), 10963. [3] Cantor, B. A.et al. (2010) Icarus, 61–81. [4] Calvin, W. M. et al. (2015) Icarus181–190. [5] Smith, I. B. et al. (2013) JGR 1835–1857. [6] Smith, I. B. and Spiga, A. (2018) Icarus, 308, 188–196. [7] Bramson et al. (2019 JGR 124, 1020–104. [8] Spiga, A. and Forget, F. (2009) JGR, 114. [9] Wolkenberg, P. et al. (2020) JGR, 125(3). [10] Plesa, A.-C. et al. (2016) JGR, 121(10), 2166–2175.\